

# Supplementary Information

## Tuning Rectification in Single-Molecular Diodes

Arunabh Batra<sup>†,1</sup>, Pierre Darancet<sup>†,1,3</sup>, Qishui Chen<sup>†,2</sup>, Jeffrey S. Meisner<sup>2,‡</sup>, Jonathan R. Widawsky<sup>1</sup>, Jeffrey B. Neaton<sup>3,\*</sup>, Colin Nuckolls<sup>2,\*</sup>, Latha Venkataraman<sup>1,\*</sup>

<sup>1</sup>*Department of Applied Physics and Applied Mathematics, Columbia University, New York, NY*

<sup>2</sup>*Department of Chemistry, Columbia University, New York, NY*

<sup>3</sup>*Molecular Foundry, Lawrence Berkeley National Laboratory, Berkeley, California, United States*

†Authors contributed equally to this work.

‡ Current address: Department of Chemistry, Duke University

\* Corresponding Authors : (JBN) neaton@lbl.gov, (CN) cn37@columbia.edu, (LV) lv2117@columbia.edu

### Table of Contents

1. Details of Chemical Synthesis
2. Synthetic Procedures
3. Experimental Methods and Data Selection
  - 3.1. Conductance and Current-Voltage (IV) Measurements
  - 3.2. Data Selection and Sorting
  - 3.3. Obtaining Statistically Most-Likely IV Curves
  - 3.4. Control Measurements
4. Density Functional Theory Calculations
5. Tight Binding Model
6. References
7. Coordinates for DFT Optimized Structures
8. NMR Spectra

## 1. Details of Chemical Synthesis

All reactions were performed in flame-dried round bottom flasks, unless otherwise noted. The flasks were fitted with rubber septa and reactions were conducted under a positive pressure of argon, unless otherwise noted. Anhydrous solvents were obtained from a Schlenk manifold with purification columns packed with activated alumina and supported copper catalyst (Glass Contour, Irvine, CA). Stainless steel syringes were used to transfer air- and moisture-sensitive liquids. Chromatography was performed on a Teledyne ISCO Combiflash RF using Redisep RF silica gel columns.

The following reagents were purchased from Sigma-Aldrich: 4-(methylthio)benzaldehyde, methyl 4-(bromomethyl)benzoate, triethyl phosphite, 3,3-dimethylallyl bromide, polyphosphoric acid, 4-nitrobenzaldehyde, thiophenol, titanium tetrachloride, zinc powder, lithium aluminum hydride, potassium *tert*-butoxide, tetrabromomethane, triphenylphosphine, *n*-butyllithium (1.6 M in hexanes), hexamethyldistannane. The following reagent was purchased from Alfa Aesar: 4-bromothiophenol.

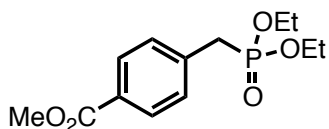
*n*-butyllithium was titrated with diphenylacetic acid prior to use.

Proton nuclear magnetic resonance ( $^1\text{H}$  NMR) spectra, carbon nuclear magnetic resonance ( $^{13}\text{C}$  NMR) spectra, tin nuclear magnetic resonance ( $^{119}\text{Sn}$  NMR) were recorded on a Bruker DRX300 (300 MHz) and Bruker DRX400 (400 MHz) spectrometer. Chemical shifts for protons are reported in parts per million downfield from tetramethylsilane and are referenced to NMR solvent ( $\text{CHCl}_3$ :  $\delta$  7.26). Chemical shifts for carbon are reported in parts per million downfield from tetramethylsilane and referenced to the carbon resonances of the solvent ( $\text{CDCl}_3$ :  $\delta$  77.2). Spectra were analyzed with MestraNova software (Version 7.1). Data are represented as follows: chemical shift, multiplicity (s = singlet, d = doublet, t = triplet, m = multiplet), coupling constants in Hertz (Hz), and integration. Mass spectroscopic data were obtained at the Columbia University mass spectrometry facility using a JEOL JMSHX110A/110A tandem mass spectrometer.

4,4-dimethylthiochroman-6-carbaldehyde (**4b**)<sup>1</sup>, (*E*)-1,2-bis(4-(methylthio)phenyl)ethene (**S1**)<sup>2</sup> were synthesized according to reported procedure.

## 2. Synthetic Procedures

### Diethyl (4-(methoxycarbonyl)benzyl)phosphonate (**P1**)



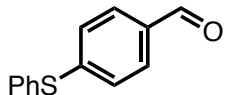
In a 25 mL round bottom flask equipped with a reflux condenser, methyl 4-(bromomethyl)benzoate (5g, 21.8 mmol) and triethyl phosphite (7.5 mL, 43.6 mmol) were stirred at 120 °C for 5 hours. Excess triethyl phosphite was then removed by vacuum distillation, and the phosphonate was obtained in 92% yield.

<sup>1</sup>H NMR (400 MHz, CDCl<sub>3</sub>): δ 7.96 (d, *J* = 7.6 Hz, 2H), 7.35 (dd, *J* = 8.2, 2.4 Hz, 2H), 3.99 (m, 4H), 3.88 (s, 3H), 3.17 (d, *J* = 22.0 Hz, 2H), 1.21 (t, *J* = 7.2 Hz, 3H).

<sup>13</sup>C NMR (101 MHz, CDCl<sub>3</sub>): δ 166.9, 137.2 (*J*<sub>C-P</sub> = 9.0 Hz), 129.9, 129.8, 128.9, 62.3 (*J*<sub>C-P</sub> = 7.0 Hz), 52.2, 34.1 (*J*<sub>C-P</sub> = 137.0 Hz), 16.4 (*J*<sub>C-P</sub> = 5.0 Hz).

HRMS (FAB+): calculated for C<sub>13</sub>H<sub>19</sub>O<sub>5</sub>P 287.1048, found 287.1039.

### 4-(phenylthio)benzaldehyde (**4c**)



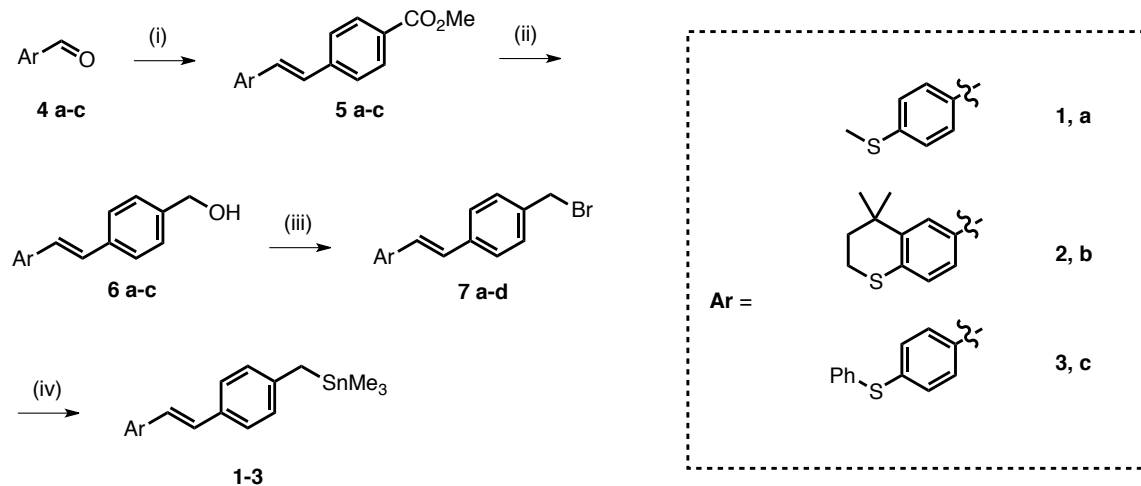
Preparation of the title compound was adapted from previously reported procedure.<sup>3</sup>

A 50 mL round bottom flask was charged with 4-nitrobenzaldehyde (1.50 g, 9.9 mmol), cesium carbonate (3.88 g, 11.9 mol), and 20 mL DMSO. Thiophenol (1.2 mL, 11.9 mmol) was added dropwise to the solution, and the reaction was stirred at room temperature for 2 h. Water (50 mL) was then added, and the mixture extracted 3 times with dichloromethane then washed with brine. The combined organic layers were dried over MgSO<sub>4</sub>, filtered, and concentrated under reduced pressure. The resulting yellow oil was purified by flash chromatography using 10% ethyl acetate in hexanes to yield an off-white solid (1.35 g, 66%). This compound matches the reported spectroscopic data.<sup>4</sup>

<sup>1</sup>H NMR (400 MHz, CDCl<sub>3</sub>): δ 9.91 (s, 1H), 7.72 (dt, *J* = 8.4 Hz, *J* = 2.0 Hz, 2H), 7.52-7.54 (m, 2H), 7.42-7.44 (m, 3H), 7.24 (dt, *J* = 8.4 Hz, *J* = 2.0 Hz, 2H).

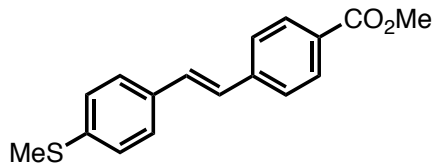
<sup>13</sup>C NMR (101 MHz, CDCl<sub>3</sub>): δ 191.3, 147.4, 134.5, 133.9, 131.5, 130.3, 130.0, 129.3, 127.4.

HRMS (FAB+): calculated for C<sub>13</sub>H<sub>10</sub>OS 214.0452, found 214.0447.



**Scheme S1: Synthesis of 1-3.** key: (i) KO<sup>t</sup>Bu, phosphonate **P1**, THF, 0 °C to r.t., 64-75% yield. (ii) LiAlH<sub>4</sub>, THF, 0 °C to r.t., 79%-86% yield. (iii) CBr<sub>4</sub>, PPh<sub>3</sub>, THF, 0 °C to r.t., 60%-67% yield. (iv) Me<sub>3</sub>SnSnMe<sub>3</sub>, *n*-BuLi, THF, -10 °C, 56%-64% yield.

#### (E)-methyl 4-(methylthio)styrylbenzoate (**5a**)



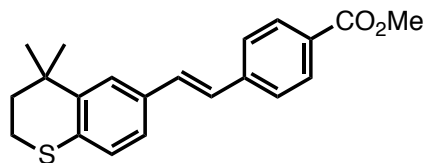
The title compound was prepared by an adaptation of a previously reported procedure.<sup>5</sup> In a flame-dried 50 mL round bottom flask, 4-(methylthio)benzaldehyde (**4a**, 620 mg, 3.0 mmol, 1 eq) and phosphonate **P1** (1.03 g, 3.6 mmol, 1.2 eq) were dissolved 15 mL anhydrous THF. The solution was cooled to 0 °C, upon which potassium *tert*-butoxide (370 mg, 3.3 mmol, 1.1 eq) in 5 mL THF was added dropwise to solution. The reaction was then warmed to room temperature. After 2 hours, water was added, and the aqueous layer was extracted with dichloromethane 3 times. The organic layers were combined, dried with magnesium sulfate, filtered, and concentrated. The residue was purified by recrystallization in THF/methanol, yielding a light yellow solid (588 mg, 64% yield).

<sup>1</sup>H NMR (400 MHz, CDCl<sub>3</sub>): δ 8.02 (d, *J* = 8.4 Hz, 2H), 7.55 (d, *J* = 8.4 Hz, 2H), 7.45 (d, *J* = 8.4 Hz, 2H), 7.25 (d, *J* = 8.4 Hz, 2H), 7.17 (d, *J* = 16.4 Hz, 1H), 7.08 (d, *J* = 16.4 Hz, 1H), 3.92 (s, 3H), 2.51 (s, 3H).

<sup>13</sup>C NMR (101 MHz, CDCl<sub>3</sub>): δ 167.0, 142.0, 139.0, 133.8, 130.7, 130.2, 129.0, 127.3, 127.0, 126.7, 126.4, 52.2, 15.8.

HRMS (FAB+): calculated for C<sub>17</sub>H<sub>16</sub>O<sub>2</sub>S 284.0871, found 284.0876.

**(E)-methyl 4-(2-(4,4-dimethylthiochroman-6-yl)vinyl)benzoate (5b)**



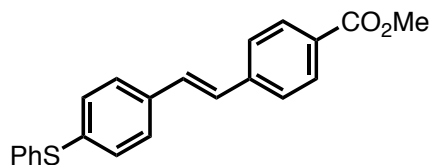
Prepared from general procedure, using **4b** instead of **4a**. The product was recrystallized from DCM/MeOH as a white solid in 75% yield.

<sup>1</sup>H NMR (400 MHz, CDCl<sub>3</sub>): δ 8.01 (d, *J* = 8.4 Hz, 2H), 7.55 (d, *J* = 8.4 Hz, 2H), 7.47 (d, *J* = 2.0 Hz, 1H), 7.26 (dd, *J* = 8.4 Hz, *J* = 2.0 Hz, 1H), 7.15 (d, *J* = 16.4 Hz, 1H), 7.09 (d, *J* = 8.4 Hz, 1H), 7.03 (d, *J* = 16.4 Hz, 1H), 3.92 (s, 3H), 3.05 (m, 2H), 1.98 (m, 2H), 1.37 (s, 6H).

<sup>13</sup>C NMR (101 MHz, CDCl<sub>3</sub>): δ 167.1, 142.4, 142.3, 132.9, 132.7, 131.4, 130.12, 128.8, 127.1, 126.3, 126.1, 125.6, 124.0, 52.2, 37.7, 33.2, 30.3, 23.4.

HRMS (FAB+): calculated for C<sub>21</sub>H<sub>22</sub>O<sub>2</sub>S 338.1341, found 338.1342.

**(E)-methyl 4-(4-(phenylthio)styryl)benzoate (5c)**



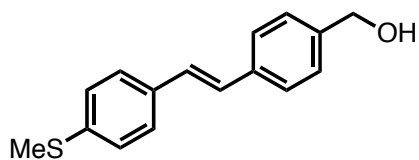
Prepared from general procedure, using **4c** instead of **4a**. The product was recrystallized from THF/MeOH as a white solid in 75% yield.

<sup>1</sup>H NMR (400 MHz, CDCl<sub>3</sub>): δ 8.02 (d, *J* = 8.4 Hz, 2H), 7.55 (d, *J* = 8.4 Hz, 2H), 7.45 (d, *J* = 8.4 Hz, 2H), 7.38-7.41 (m, 2H), 7.28-7.35 (m, 5H), 7.17 (d, *J* = 16.4 Hz, 1H), 7.10 (d, *J* = 16.4 Hz, 1H), 3.92 (s, 3H).

<sup>13</sup>C NMR (101 MHz, CDCl<sub>3</sub>): δ 167.0, 141.8, 136.4, 135.6, 135.3, 131.7, 130.9, 130.5, 130.2, 129.5, 129.1, 127.9, 127.6, 127.6, 126.5, 52.3.

HRMS (FAB+): calculated for C<sub>22</sub>H<sub>18</sub>O<sub>2</sub>S 346.1028, found 346.1026.

**(E)-(4-(4-(methylthio)styryl)phenyl)methanol (6a)**



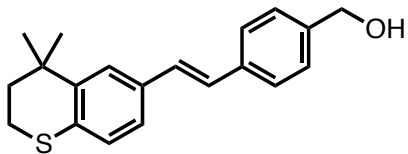
A 100 mL flame-dried round bottom flask was charged with **5a** (500 mg, 1.75 mmol). The white solid was fully dissolved in 20 mL THF, then cooled to 0 °C in an ice bath. LiAlH<sub>4</sub> (133 mg, 3.50 mmol) in 5 mL THF, which is a gray slurry, was added dropwise to the solution. The reaction was then warmed to room temperature and monitored by TLC to determine the consumption of starting material. After 30 minutes, the conversion was complete by TLC. The reaction was quenched by careful, dropwise addition of water. The aqueous and organic layers were separated, and the aqueous layer was extracted twice with dichloromethane. The combined organic layers were dried with magnesium sulfate, filtered, and concentrated to yield an off-white solid, which was washed with hexanes and dried. Yield: 391 mg, 86%.

<sup>1</sup>H NMR (400 MHz, CDCl<sub>3</sub>): δ 7.50 (d, *J* = 8.4 Hz, 2H), 7.44 (d, *J* = 8.4 Hz, 2H), 7.36 (d, *J* = 8.4 Hz, 2H), 7.24 (d, *J* = 8.4 Hz, 2H), 7.06 (s, 2H), 4.70 (s, 2H), 2.51 (s, 3H).

<sup>13</sup>C NMR (101 MHz, CDCl<sub>3</sub>): δ 140.3, 138.1, 137.0, 134.4, 128.3, 127.8, 127.5, 127.0, 126.9, 126.8, 65.3, 16.0.

HRMS (FAB+): calculated for C<sub>16</sub>H<sub>16</sub>OS 256.0922, found 256.0927.

**(E)-(4-(2-(4,4-dimethylthiochroman-6-yl)vinyl)phenyl)methanol (6b)**



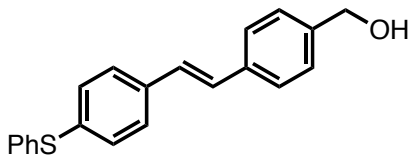
Prepared from general procedure, using **5b** instead of **5a**. The product was recrystallized from dichloromethane/hexanes as a white solid. Yield: 79%.

<sup>1</sup>H NMR (400 MHz, CDCl<sub>3</sub>): δ 7.50 (d, *J* = 8.4 Hz, 2H), 7.46 (d, *J* = 2.0 Hz, 1H), 7.35 (d, *J* = 8.4 Hz, 2H), 7.24 (dd, *J* = 8.4 Hz, *J* = 2.0 Hz, 1H), 7.08 (d, *J* = 8.4 Hz, 1H), 7.06 (d, *J* = 16.4 Hz, 1H), 7.01 (d, *J* = 16.4 Hz, 1H), 4.70 (s, 2H), 3.05 (m, 2H), 1.98 (m, 2H), 1.37 (s, 6H).

<sup>13</sup>C NMR (101 MHz, CDCl<sub>3</sub>): δ 142.3, 140.1, 137.2, 133.4, 131.7, 128.9, 127.5, 127.0, 126.8, 126.7, 125.3, 123.8, 65.4, 37.8, 33.2, 30.3, 23.3.

HRMS (FAB+): calculated for C<sub>20</sub>H<sub>22</sub>OS 310.1391, found 310.1397.

#### (E)-(4-(4-(phenylthio)styryl)phenyl)methanol (**6c**)



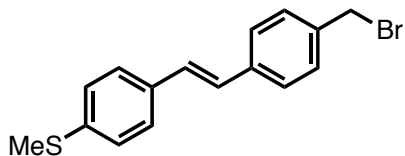
Prepared from general procedure, using **5c** instead of **5a**. The product was recrystallized from dichloromethane/hexanes as a white solid. Yellow solid. Yield: 82%.

<sup>1</sup>H NMR (400 MHz, CDCl<sub>3</sub>): δ 7.51 (d, *J* = 8.4 Hz, 2H), 7.44 (d, *J* = 8.4 Hz, 2H), 7.36-7.37 (m, 4H), 7.27-7.33 (m, 5H), 7.10 (d, *J* = 16.4 Hz, 1H), 7.06 (d, *J* = 16.4 Hz, 1H), 4.71 (s, 2H).

<sup>13</sup>C NMR (101 MHz, CDCl<sub>3</sub>): δ 140.5, 136.8, 136.3, 135.2, 131.3, 131.2, 129.4, 128.8, 128.0, 127.6, 127.3, 127.3, 126.9, 100.1, 65.3.

HRMS (FAB+): calculated for C<sub>21</sub>H<sub>18</sub>OS 318.1078, found 318.1081.

**(E)-(4-(4-(bromomethyl)styryl)phenyl)(methyl)sulfane (7a)**



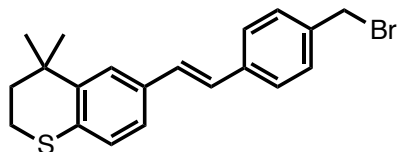
In a 100 mL round bottom flask, **6a** (256 mg, 1.00 mmol) and CBr<sub>4</sub> (995 mg, 3.00 mmol) were dissolved in 30 mL THF, and cooled to 0 °C in an ice bath. Triphenylphosphine (787 mg, 3.00 mmol) in 5 mL THF was slowly added. The reaction was then warmed to temperature, and a white precipitate (triphenylphosphine oxide) gradually forms. In 1 hour, the reaction was filtered through a celite pad, then concentrated to obtain a light yellow semi-solid. The residue was washed with methanol and filtered to obtain an off-white solid (214 mg, 67% yield).

<sup>1</sup>H NMR (400 MHz, CDCl<sub>3</sub>): δ 7.47 (d, *J* = 8.4 Hz, 2H), 7.43 (d, *J* = 8.4 Hz, 2H), 7.38 (d, *J* = 8.4 Hz, 2H), 7.24 (d, *J* = 8.4 Hz, 2H), 7.08 (d, *J* = 16.4 Hz, 1H), 7.03 (d, *J* = 16.4 Hz, 1H), 4.52 (s, 2H), 2.51 (s, 3H).

<sup>13</sup>C NMR (101 MHz, CDCl<sub>3</sub>): δ 138.4, 137.8, 137.1, 134.2, 129.6, 129.0, 127.4, 127.1, 126.9, 126.9, 33.7, 15.9.

HRMS (FAB+): calculated for C<sub>16</sub>H<sub>15</sub>BrS 318.0078, found 318.0085.

**(E)-6-(4-(bromomethyl)styryl)-4,4-dimethylthiochroman (7b)**



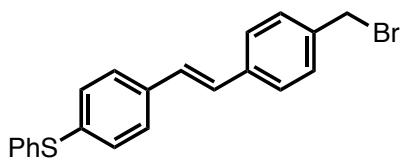
Prepared from general procedure, using **6b** instead of **6a**. The product was recrystallized from toluene/methanol as a white solid in 60% yield.

<sup>1</sup>H NMR (400 MHz, CDCl<sub>3</sub>): δ 7.45-7.47 (m, 3H), 7.37 (d, *J* = 8.4 Hz, 2H), 7.24 (dd, *J* = 8.4 Hz, *J* = 2.0 Hz, 1H), 7.08 (d, *J* = 8.4 Hz, 1H), 7.05 (d, *J* = 16.4 Hz, 1H), 7.00 (d, *J* = 16.4 Hz, 1H), 4.52 (s, 2H), 3.05 (m, 2H), 1.98 (m, 2H), 1.37 (s, 6H).

<sup>13</sup>C NMR (101 MHz, CDCl<sub>3</sub>): δ 142.3, 138.0, 136.8, 133.2, 132.0, 129.63, 129.59, 127.1, 126.8, 126.5, 125.4, 123.9, 37.7, 33.8, 33.2, 30.3, 23.3.

HRMS (FAB+): calculated for C<sub>20</sub>H<sub>21</sub>BrS 372.0547, found 372.0543.

**(E)-(4-(bromomethyl)styryl)phenyl(phenyl)sulfane (7c)**



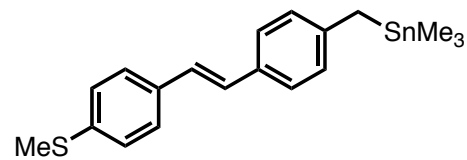
Prepared from general procedure, using **6c** instead of **6a**. The product was recrystallized from toluene/methanol as a light yellow solid in 63% yield.

<sup>1</sup>H NMR (400 MHz, CDCl<sub>3</sub>): δ 7.47 (d, *J* = 8.4 Hz, 2H), 7.44 (d, *J* = 8.4 Hz, 2H), 7.37-7.39 (m, 4H), 7.25-7.34 (m, 5H), 7.07 (s, 2H), 4.51 (s, 2H).

<sup>13</sup>C NMR (101 MHz, CDCl<sub>3</sub>): δ 137.5, 137.3, 136.1, 135.7, 135.6, 131.4, 131.2, 129.6, 129.4, 128.7, 128.4, 127.4, 127.4, 127.0, 33.6.

HRMS (FAB+): calculated for C<sub>21</sub>H<sub>17</sub>BrS 380.0234, found 380.0224.

**(E)-trimethyl(4-(4-(methylthio)styryl)benzyl)stannane (1)**



Trimethylstannyllithium was prepared from hexamethyldistannane and *n*-BuLi adapted from known literature procedure.<sup>6</sup> A flame-dried 25 mL Schlenk flask was charged with hexamethyldistannane (115 mg, 0.35 mmol) and 10 mL anhydrous THF under argon. The solution was cooled to -10 °C, and freshly titrated *n*-BuLi (1.53 M, 0.21 mL, 0.32 mmol)

was added dropwise. After stirring for 1 h, an aliquot was quenched with benzyl bromide, and formation of the desired stannane was confirmed by  $^1\text{H}$  NMR. **7a** (50 mg, 0.16 mmol) and 2 mL THF were added to a separate flame-dried 25 mL Schlenk flask and cooled to -10 °C with stirring. Trimethylstannyllithium solution was cannulated dropwise to the cooled solution of **7a**. The reaction was warmed to room temperature and stirred for 1 h, after which water was slowly added, and the mixture was extracted with dichloromethane 3 times. The organic layers were combined, dried with magnesium sulfate, filtered, and concentrated. Preparative thin layer chromatography eluting with hexanes: ethyl acetate: triethylamine = 9:1:0.1 yielded a light yellow solid (37 mg, 58%).

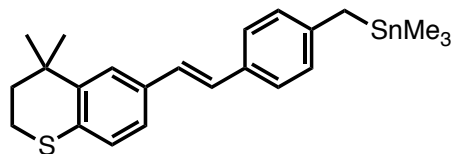
$^1\text{H}$  NMR (400 MHz,  $\text{CDCl}_3$ ):  $\delta$  7.41 (d,  $J$  = 8.4 Hz, 2H), 7.34 (d,  $J$  = 8.4 Hz, 2H), 7.23 (d,  $J$  = 8.4 Hz, 2H), 7.02 (d,  $J$  = 16.4 Hz, 1H), 6.96 (d,  $J$  = 8.4 Hz, 2H), 6.96 (d,  $J$  = 16.4 Hz, 1H), 2.50 (s, 3H), 2.33 (m, 2H), 0.06 (m, 9H).

$^{13}\text{C}$  NMR (101 MHz,  $\text{CDCl}_3$ ):  $\delta$  143.3, 137.3, 135.0, 132.5, 128.5, 127.2, 127.0, 126.8, 126.7, 126.1, 20.5, 16.1, -9.8.

$^{119}\text{Sn}$  NMR (112 MHz,  $\text{CDCl}_3$ ):  $\delta$  5.26.

HRMS (FAB+): calculated for  $\text{C}_{19}\text{H}_{24}\text{S}^{116}\text{Sn}$  404.0621, found 404.0620.

#### (E)-(4-(2-(4,4-dimethylthiochroman-6-yl)vinyl)benzyl)trimethylstannane (**2**)



Prepared from general procedure, using **7b** instead of **7a**. The product was purified by preparative thin layer chromatography eluting with hexanes: ethyl acetate: triethylamine = 9:1:0.1 to yield a light yellow solid. Yield: 64%.

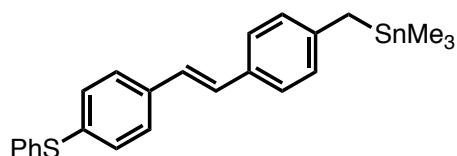
$^1\text{H}$  NMR (400 MHz,  $\text{CDCl}_3$ ):  $\delta$  7.43 (d,  $J$  = 2.0 Hz, 1H), 7.33 (d,  $J$  = 8.4 Hz, 2H), 7.20 (dd,  $J$  = 8.4 Hz,  $J$  = 2.0 Hz, 1H), 7.05 (d,  $J$  = 8.4 Hz, 1H), 6.95-6.97 (m, 4H), 3.04 (m, 2H), 2.33 (m, 2H), 1.97 (m, 2H), 1.37 (s, 6H), 0.06 (m, 9H).

<sup>13</sup>C NMR (101 MHz, CDCl<sub>3</sub>): δ 143.0, 142.2, 134.0, 132.7, 131.0, 127.5, 127.2, 127.0, 126.8, 126.6, 125.1, 123.7, 37.9, 33.2, 30.4, 23.3, 20.5, -9.8.

<sup>119</sup>Sn NMR (112 MHz, CDCl<sub>3</sub>): δ 4.99.

HRMS (FAB+): calculated for C<sub>23</sub>H<sub>30</sub>S<sup>116</sup>Sn 454.1090, found 454.1091.

**(E)-trimethyl(4-(phenylthio)styryl)benzyl)stannane (3)**



Prepared from general procedure, using **7c** instead of **7a**. The product was purified by preparative thin layer chromatography eluting with hexanes: ethyl acetate: triethylamine = 9:1:0.1 to yield a light yellow solid. Yield: 56%.

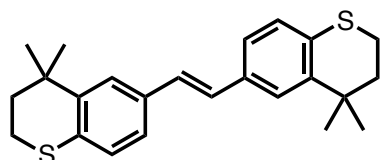
<sup>1</sup>H NMR (400 MHz, CDCl<sub>3</sub>): δ 7.42 (d, *J* = 8.4 Hz, 2H), 7.28-7.36 (m, 8H), 7.23-7.24 (m, 1H), 7.05 (d, *J* = 16.4 Hz, 1H), 6.97 (d, *J* = 8.4 Hz, 2H), 6.96 (d, *J* = 16.4 Hz, 1H), 2.33 (m, 2H), 0.06 (m, 9H).

<sup>13</sup>C NMR (101 MHz, CDCl<sub>3</sub>): δ 143.6, 137.0, 136.2, 134.2, 132.3, 131.7, 130.9, 129.5, 129.3, 127.2, 127.1, 127.1, 126.8, 125.8, 20.6, -9.8.

<sup>119</sup>Sn NMR (112 MHz, CDCl<sub>3</sub>): δ 5.49.

HRMS (FAB+): calculated for C<sub>24</sub>H<sub>26</sub>S<sup>116</sup>Sn 462.0773, found 462.0777.

**(E)-1,2-bis(4,4-dimethylthiochroman-6-yl)ethene (S2)**



The title compound was synthesized by an adaptation of a previously reported procedure.<sup>7</sup> A flame-dried 100 mL two-neck flask was charged with zinc powder (392 mg, 6.00 mmol) and 20 mL anhydrous THF. The suspension was cooled to -0 °C, and

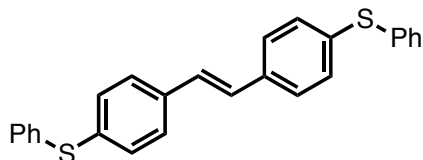
titanium tetrachloride (3.00 mmol, 0.33 mL) was added dropwise. The flask was sealed with a reflux condenser and heated to reflux for 90 minutes, during which the solution was observed to darken. This mixture was then cooled in an ice bath to -0 °C, and **4b** (2.00 mmol, 413 mg) in 10 mL anhydrous THF was added dropwise. The reaction was heated to reflux for 12 h. After cooling to room temperature, the mixture was slowly poured into 20 mL saturated sodium bicarbonate solution and stirred for 2 h. The aqueous and organic layers were separated, and the aqueous layer was extracted with ethyl acetate. The organic layers were combined, dried with magnesium sulfate, filtered, and concentrated. The residue was purified by recrystallization in THF/MeOH, yielding a white solid (183 mg, 48% yield).

<sup>1</sup>H NMR (400 MHz, CDCl<sub>3</sub>): δ 7.44 (d, *J* = 2.0 Hz, 2H), 7.22 (dd, *J* = 8.4 Hz, *J* = 2.0 Hz, 2H), 7.06 (d, *J* = 8.4 Hz, 2H), 6.95 (s, 2H), 3.05 (m, 4H), 1.98 (m, 4H), 1.37 (s, 12H).

<sup>13</sup>C NMR (101 MHz, CDCl<sub>3</sub>): δ 142.2, 133.7, 131.2, 127.3, 127.0, 125.1, 123.7, 37.8, 33.2, 30.3, 23.3.

HRMS (FAB+): calculated for C<sub>24</sub>H<sub>28</sub>S<sub>2</sub> 380.1632, found 310.1648.

**(E)-1,2-bis(4-(phenylthio)phenyl)ethene (S3)**



Prepared from general procedure, using **4c** instead of **4b**. The product was recrystallized from THF/MeOH as a white solid in 39% yield.

<sup>1</sup>H NMR (400 MHz, CDCl<sub>3</sub>): δ 7.43 (d, *J* = 8.4 Hz, 2H), 7.25-7.38 (m, 14H), 7.05 (s, 2H).

<sup>13</sup>C NMR (101 MHz, CDCl<sub>3</sub>): δ 136.15, 135.71, 135.48, 131.33, 131.25, 129.40, 128.30, 127.36, 127.33.

HRMS (FAB+): calculated for C<sub>26</sub>H<sub>20</sub>S<sub>2</sub> 396.1006, found 396.1017.

### **3. Experimental Methods and Data Selection**

#### *3.1 Conductance and IV Measurements*

Molecular conductance is measured by repeatedly forming and breaking gold point contacts in a solution of molecules with a custom Scanning Tunneling Microscope (STM)<sup>8</sup>. A freshly cut gold wire (0.25 mm diameter, 99.999% purity, Alfa Aesar) is used as the tip, and UV/ozone cleaned gold substrate (mica with 100 nm gold, 99.999% purity, Alfa Aesar) is used as the substrate. The STM operates in ambient conditions at room temperature, and the junctions are broken in dilute (1mM to 10mM) solutions of molecules in 1,2,4-trichlorobenzene (Sigma-Aldrich, 99% purity). Before adding a molecular solution, 1,000 conductance traces are first collected to ensure that there are no contaminations in the STM set-up. Current-voltage (IV) measurements are carried out using previously published methods<sup>9</sup>. Briefly, the STM tip is brought into contact with the substrate until a junction conductance of  $>5G_0$  ( $G_0 = 77.6 \mu\text{S}$ ) is measured. The tip is then withdrawn at a rate of 15 nm/s for 125 ms, and held at this displacement for 150 ms before being withdrawn for an additional 75 ms. During the ‘hold’ section, the applied voltage is ramped between  $\pm 1\text{V}$ , while current and voltage are measured simultaneously (Figure 1b in the main text). Traces that show a molecular signature through the entirety of the IV ramp are selected as successful IV traces. In general, 1-10% of measured junctions are selected from  $\sim 50,000$  measured traces per experiment. Data from multiple experiments is added together to form the histograms shown in the main text, with each histogram containing  $>2000$  successful IV traces.

#### *3.2 Data Selection and Sorting*

The procedure for selection of successful IV traces is shown in Figure S1a. As mentioned in the main text, each recorded trace contains a 150 ms ‘hold’ section, where the tip-substrate separation is kept fixed while the tip-substrate voltage is ramped. Since not all recorded traces include a conductance plateau corresponding to the molecule, data selection is performed on select traces with a molecular conductance signature that is stable before and after the application of an IV ramp. Average conductance is calculated

25ms before ( $\bar{G}_{pre}$ ) and after ( $\bar{G}_{post}$ ) the IV ramp, and for 10ms at the middle of the ramp ( $\bar{G}_{mid}$ ). At these portions of the trace, the junction is in zero-bias conditions ( $V_{\text{applied}} < 100$  mV). Selected curves must have  $\bar{G}_{pre}$ ,  $\bar{G}_{post}$  and  $\bar{G}_{mid}$  within the full-width at half maximum (FWHM) of the peak in the conductance histogram measured at low bias. This procedure typically selects between 1-10% of measured traces, which can then be used to make two-dimensional (2D) IV histograms using either linear or log binning. Figure 1c in the main text shows an example of such a 2D histogram using linear binning.

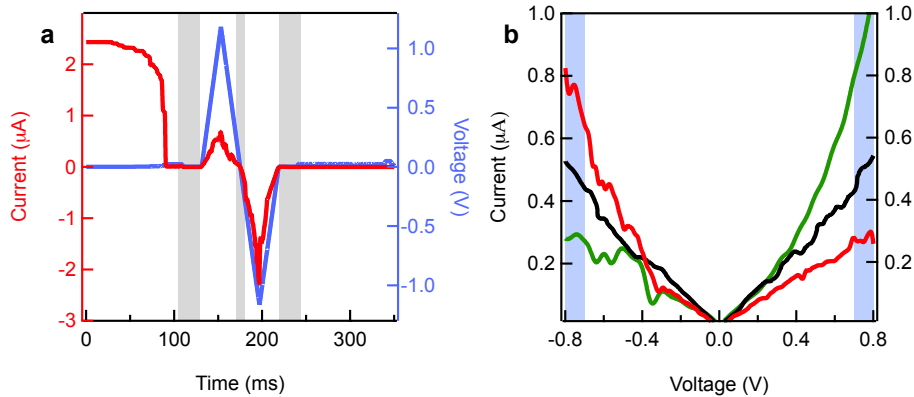


**Figure S1: Data selection and sorting methods.** **a** Sample trace showing measured current (red) and applied voltage (blue) on a molecular junction. A trace is considered a stable molecular junction if measured conductances before, during and after voltage ramp (shaded regions) are at the characteristic zero-bias conductance of the molecule. **b** The presented sample IV curves are representative of the three types of IV curves, forward bias (green), reverse bias (red), and non-rectifying (black). IV curves are sorted by comparing magnitudes of average current ( $I$ ) at positive and negative biases (blue shaded regions).

Selected data can be sorted (all selected traces are used) based on magnitude of current at positive and negative voltages, resulting in separated histograms shown in Figure 1d and 1e in the main text. The data sorting procedure is outlined in Figure S1b. Measured current is averaged between +0.75 V and +0.80 V ( $\bar{I}_{pos}$ ) and -0.75V to -0.80V ( $\bar{I}_{neg}$ ). If  $abs(\bar{I}_{pos}) > abs(\bar{I}_{neg})$ , the junction is considered to be in the forward bias condition, and vice versa. Based on this selection process, the data are sorted into two 2D histograms (such as Figure 1d and 1e) that are then used to obtain a ‘statistically most

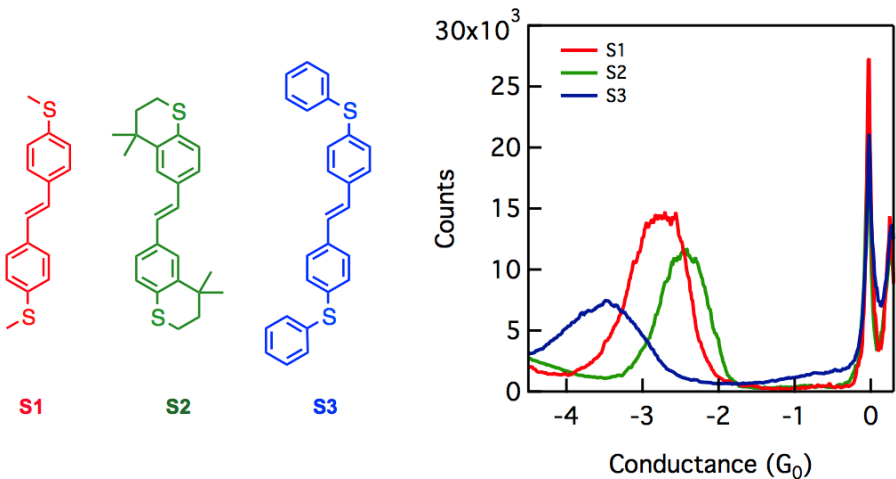
likely' (hereafter called average IV curve) IV curve for forward and reverse bias conditions. The results of sorting do not change appreciably if the voltage selection window (blue shaded regions in Figure S1b) is widened or moved to slightly lower or higher ranges. The three example traces shown in Figure S1b are characteristic of IV curves observed in experiments. In this case, the green curve and red curve are selected into forward and reverse bias histograms respectively. Symmetric IV curves like the black curve are also observed, where the rectification ratio is comparable to stochastic variability of junction conductance. These traces are equally likely to be in the forward or reverse bias histograms and do not significantly change the resulting 2D histograms.

### 3.3 Obtaining Statistically Most-Likely IV Curves

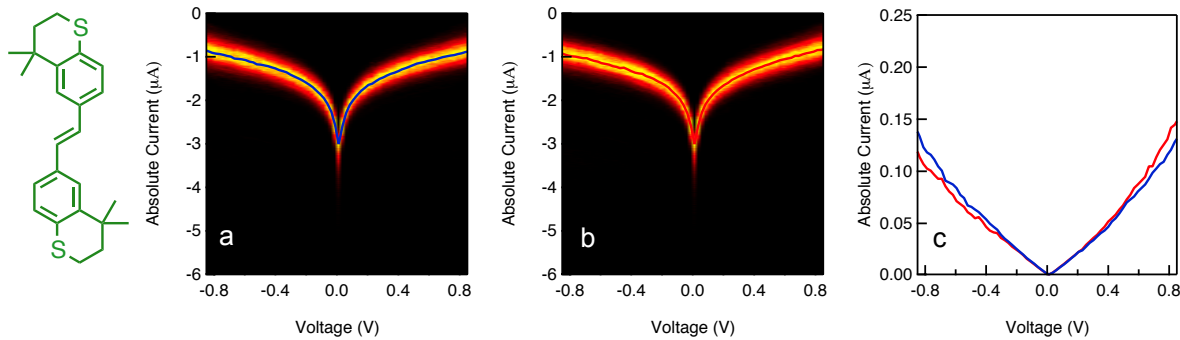
'Average' IV curves are obtained by fitting the distribution of currents at each voltage bin of a histogram (i.e. a vertical 'voltage slice' of a 2D IV histogram) to a log-normal (log-binned 2D histograms) or Gaussian (linear-binned 2D Histogram) curve; the peak of this curve represents the statistically most likely current for that voltage. This procedure is repeated for each voltage slice to generate an average IV curve (like those shown in Figure 1f). Whenever a comparison is made of IV curves between different molecules with varying conductances, it is preferable to bin current values on a logarithmic scale, while maintaining linear scaling for voltage bins. This binning scheme allows the histograms of all compared molecules to have the same ranges and bin-widths, making quantitative comparisons easier. IV curves shown in Figure 3 follow this logarithmic current binning procedure.

### 3.4 Control Molecules

Molecules **S1**, **S2** and **S3** (Figure S2a) are symmetrically linked with methylsulfide linkers corresponding to the diodes **1**, **2** and **3**. The low-bias conductance histograms of the three molecules (Figure S2b), show that conductance of **S2** > **S1** > **S3**, similar to the trend observed in the corresponding asymmetric diodes.



**Figure S2: Symmetric Controls.** **a** Chemical structures of symmetrically linked versions of rectifiers **1,2**, and **3** **b** Zero-bias conductance histograms of molecules **S1**, **S2**, and **S3**, showing that conductance of **S2**>**S1**>**S3**.



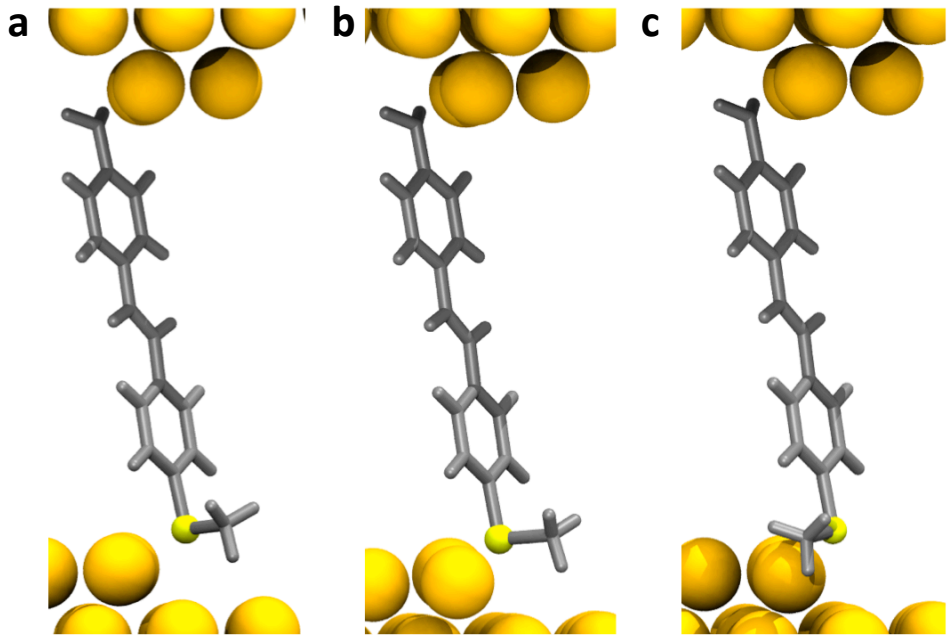
**Figure S3: IV Curves for Symmetric Control Molecules.** **a** Log-binned two dimensional IV curve histograms for molecule **S2** (drawn in green) as measured (unsorted). The blue line is a best fit, representing the statistically most likely IV curve. **b** The same data as Figure S4a, now sorted by rectification direction of each trace. Traces showing higher current at negative biases are reflected about the y-axis. The red curve shows the statistically most likely IV curve after sorting. **c** Comparison of unreflected (blue) and reflected (red) curves for molecule **S2** on a linear scale, showing that neither red nor blue curves show much rectification (<1.2 at 0.85 V), as expected for a symmetric molecule.

Figure S3a and S3b show IV histograms for molecule **S2** without and with the sorting procedure applied. We extract averaged IV curves for sorted molecules (red curves in Figure S3c), and compare with unsorted data (blue curve). The rectification ratios recovered is 1.2, which is much smaller than those found for asymmetric diode designs. The small rectification is possibly due to junction-to-junction variability in the asymmetry of the coupling of the molecule to the two electrodes.

## 4. Density Functional Theory Calculations

### 4.1 Calculation Details

We use density functional theory (DFT) as implemented in the SIESTA package<sup>10, 11</sup>. Self-consistent charge densities are obtained with localized numerical orbitals and a 300 Ry grid cutoff, a 0.05 eV electronic smearing, on a 4x4 k-point sampling in directions perpendicular to the junction. Hellmann-Feynman forces on the atoms are reduced to 0.04 eV/Å or less using a GGA-PBE<sup>12</sup> functional using a double- $\zeta$ -basis set. We use a motif consisting of 3 gold adatoms (trimer) on both sides connected to 7 layers of 16 gold atoms on either side, the last 4 layers being constrained to the bulk (PBE) geometry. Initial junction geometries for molecule **1** are chosen from previous work on carbon-gold bonded<sup>6</sup> and methylsulfide-bonded<sup>13</sup> molecules linked to under-coordinated gold. Angular dependence of the analogs of molecule **1** (figure S4) are obtained by fixing the dihedral angle of gold-carbon-phenyl to the desired values, and, and then repeating the optimization procedure. Obtained geometries are shown in figure S4, and XYZ coordinates are enclosed in section 7.



**Figure S4: DFT Optimized Geometries.** **a** Equilibrium geometry for molecule **1** connected in a junction with trimer tips. The torsional angle for the methyl-S-C-C bond is  $\theta=73^\circ$ . **b** constrained geometry with methyl group on the methylsulfide linker pointing out of the plane of the stilbene backbone ( $\theta=90^\circ$ ) **c** methyl group constrained to be in plane ( $\theta=0^\circ$ )

#### 4.2 Procedures for Density matrices and Transmission

We obtain the zero- and finite-bias density matrices using a parameter-free scattering-state approach based on DFT as implemented in the SCARLET package<sup>14</sup>. Isosurface plots of the eigenchannel wavefunctions corresponding to the major maxima in the transmission function are shown in Figure S5. Following previous works<sup>15-18</sup>, we determine the zero-bias conductance and IV characteristics from the Landauer formula. Junction geometries consist of 7 layers of 16 gold atoms on both sides. Densities and potentials are fixed to their bulk values in the 4 outermost layers on each side, and allowed to vary elsewhere. We obtain the self-consistent steady-state density matrix from DFT-PBE<sup>12</sup> as described in Darancet, Widawsky, Choi, Venkataraman and Neaton<sup>17</sup> using an 8x8  $k_{\parallel}$ -mesh. For finite bias calculations, the density matrix includes a real axis

integration of the scattering-states in the bias window on an adaptive energy grid with a resolution of up to  $10^{-7}$  eV in the vicinity of the molecular resonances. For all junctions and biases, the bias-dependent transmission functions are subsequently calculated using a  $16 \times 16 k_{\parallel}$ -mesh and an 800-point energy grid in the energy range ( $E_F - 2$ eV,  $E_F + 2$ eV). The current at a given bias is obtained through integration of the corresponding transmission function between the leads' chemical potentials. Changes in the geometries upon application of bias are neglected.

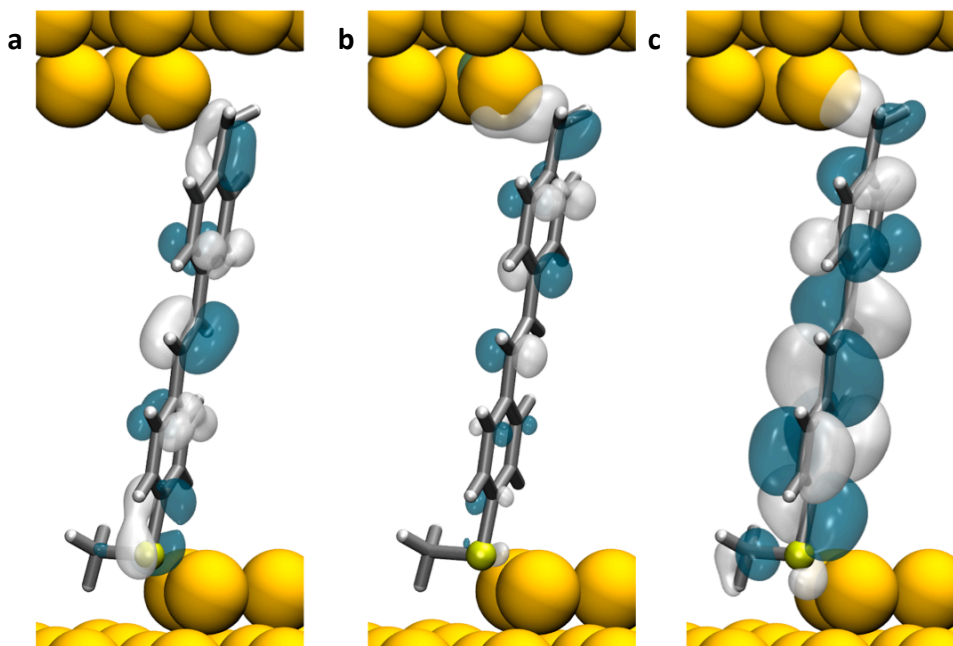


**Figure S5: Scattering states for molecule 1:** Isosurface plots of eigenchannel wavefunctions for molecule 1 at **a** -1.4 eV (HOMO), **b**  $E_F$ , and **c** 1.8 eV (LUMO). The scattering state at  $E_F$  has both ‘gateway’ state character and molecular orbital character, indicating the strong coupling between the gold-carbon bond and the backbone.

The Hartree potential for the junctions under bias is calculated by solving a Laplace equation with boundary conditions given by the Hartree potential of the bulk shifted by  $\pm \frac{V}{2}$ . The potential profile is obtained by subtracting the finite-bias Hartree potential from its zero-bias counterpart. Figure S6 shows such potential profiles averaged in the x and y directions for different biases for a junction with molecule **1**, where the potential drop across the junction is non-linear and asymmetric in the molecular region (position from -6 Å to 6 Å). The lineshape of the potential drop is bias-independent (50mV to 1V) and is a consequence of a relatively large and inhomogeneous dielectric response function of the molecule in the junction.

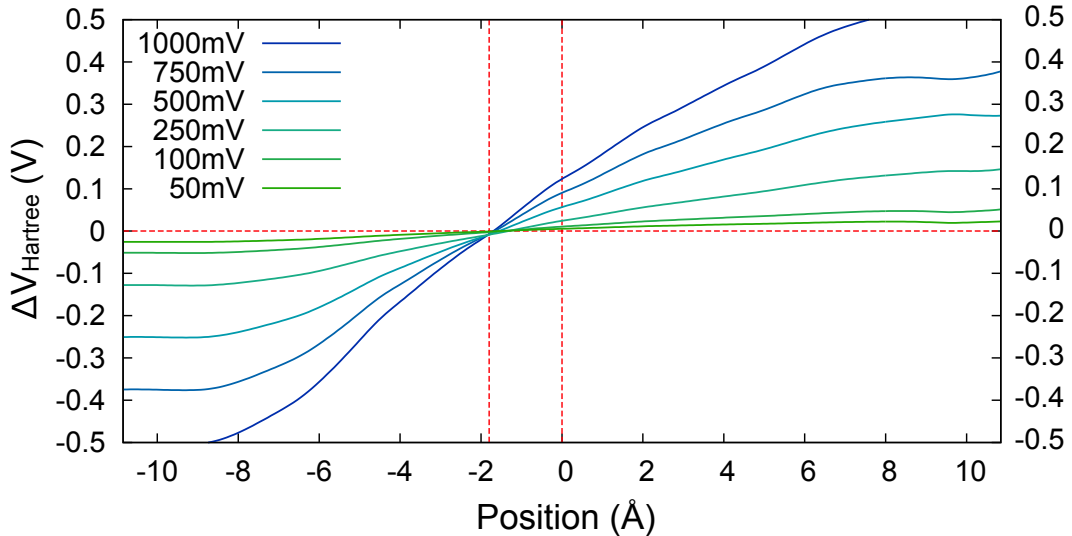


**Figure S6: Potential profile for molecule 1 at 50mV to 1V.** The potential drop in the molecular region -6 Å to 6 Å is non-linear and inhomogeneous at all biases. These profiles are calculated taking the differences in the self-consistent Hartree potentials at finite bias with respect to the zero-bias case, and averaging them in the x and y directions. The two vertical dashed lines point to asymmetry in junction. The position along the z-direction is indicated with respect to the mid-point of the gold electrodes' first layers.

Figure S7 shows the potential profile at 750mV as compared with the structure of the junction. 60% of the potential drops on the methylsulfide moiety while the potential is essentially flat in the carbon-gold region (10% decrease at this contact, 23% at the methylsulfide contact). This indicates a relatively higher local polarizability of the

carbon-gold moiety. It is worth noting that such non-linearities and inhomogeneity in the potential drop do not appear when the molecule is in the gas-phase and are a consequence of strong hybridization of the molecule with the gold electrode through the carbon-gold bond.

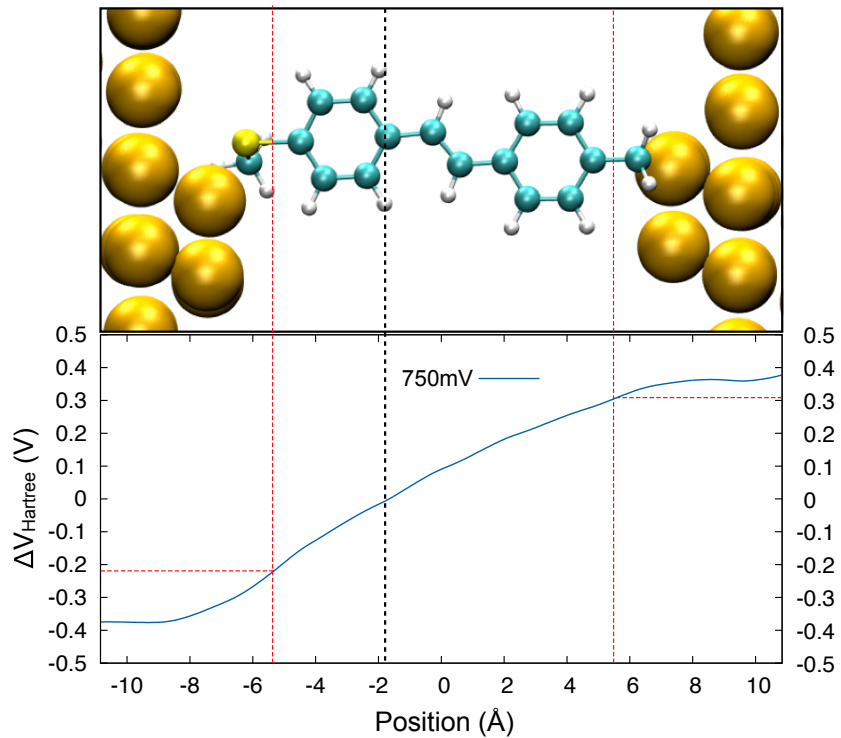


**Figure S7: Potential profile across molecular diode:** The potential profile is shown for molecule 1 in a junction with 750 mV bias. The red dashed lines indicate midpoints of sulfur carbon-bond and carbon-carbon bonds. The voltage drop at the midpoint of the sulfur-gold bond is over two times more than that at the midpoint of carbon-carbon bond on the carbon-gold bound side. The black dashed line near the center of the plot shows the zero potential point, which is shifted towards the methylsulfide side of the molecule.

## 5. Tight Binding Model

All tight-binding calculations are conducted using a bias dependent two-site model Hamiltonian  $H$  of the form

$$H(V) = \begin{bmatrix} \varepsilon_0 + \alpha_0 eV & \tau \\ \tau & \varepsilon_1 + \alpha_1 eV \end{bmatrix}$$

where  $\varepsilon_0$  is the on-site energy of the molecular orbital connected to the electrode via the carbon-gold bond, and  $\varepsilon_1$  is the on-site energy of the orbital coupled to gold through the sulfur-gold bond. Due to the very good coupling between the gold-carbon and  $\pi$ -system (shown in the scattering states of the main text and SI), state 0 can be understood as a linear combination of orbitals lying on the  $\pi$ -system (backbone) and the gateway on the gold-carbon bond, while state 1 corresponds to the methylsulfide group.  $\alpha_0$  and  $\alpha_1$  are the corresponding dimensionless constants controlling the change in the on-site energy upon application of a bias. Following Darancet, Widawsky, Choi, Venkataraman and Neaton<sup>17</sup>, for orbitals breaking inversion symmetry, we approximate this change by its first order variation (linear stark shift) with applied bias.  $\tau$  represents the coupling between states 0 and 1 and is therefore seen as the coupling between the left and right side of the junction.

A schematic representation of the model is shown in figure S7a. Retarded Green's functions, i.e.  $G(E, V) = [E - H(V) - \Sigma_L - \Sigma_R]^{-1}$  are generated from this Hamiltonian, where  $\Sigma_{L,R}$  are the self-energies of the left and right electrodes. We simplify our system by assuming that the self-energy matrices are energy independent, and that the real parts of the self-energies are negligible<sup>19</sup>. The effective Green's function then becomes:

$$G(E, V) = \begin{bmatrix} E - \varepsilon_0 - \alpha_0 eV + \frac{i\Gamma_1}{2} & \tau \\ \tau & E - \varepsilon_1 - \alpha_1 eV + \frac{i\Gamma_2}{2} \end{bmatrix}^{-1}$$

where  $\Gamma_L$  and  $\Gamma_R$  are the coupling strengths of the molecular levels to left and right Au electrodes, respectively. The transmission is then given by  $T(E, V) = [\Gamma_L G(E, V) \Gamma_R G(E, V)^\dagger]$ . Initial guesses for the parameters are taken from previous work on modeling gold-carbon bond linkers<sup>20</sup>, methylsulfide-gold contacts<sup>13</sup>, and DFT based transmission calculations presented for molecule **1** in the main text. The parameters are then optimized to match the zero bias conductance for molecule **1**; see Table ST1 for parameters used in this work. Next, IV curves are generated using the

Landauer formula,  $I(V) = \frac{2e}{h} \int dE T(E, V) \left[ f\left(E + \frac{eV}{2}\right) - f\left(E - \frac{eV}{2}\right) \right]$ , where  $f$  is the Fermi distribution function. Further parameter optimization is performed to match  $\frac{dI}{dV}$  and  $\frac{d^2I}{dV^2}$  characteristics of the experimental IV curve from molecule **1**. The resulting fit (red markers, Figure S7b) show that the model captures the essential features of the experimental IV, including the linearity of the reverse bias region and the nonlinearity of forward bias. Varying the model parameters suggested that  $\tau$ , the coupling between the left and right side of the molecule, is a critical parameter in controlling rectification ratio. This understanding allowed us to develop synthetic methods of achieving this goal, resulting in designs for molecules **2** and **3**. The experimental results from IV measurements on molecules **2** and **3**, are also well captured by changing three parameters, using the zero-bias conductance and  $\frac{dI}{dV}$  and  $\frac{d^2I}{dV^2}$  of experimental IV curves as fitting parameters. The resulting fits to the IV curves are shown in figure S7b, with tight-binding calculated transmission functions shown in figure S8. The parameters used for these results are tabulated in Table ST1.

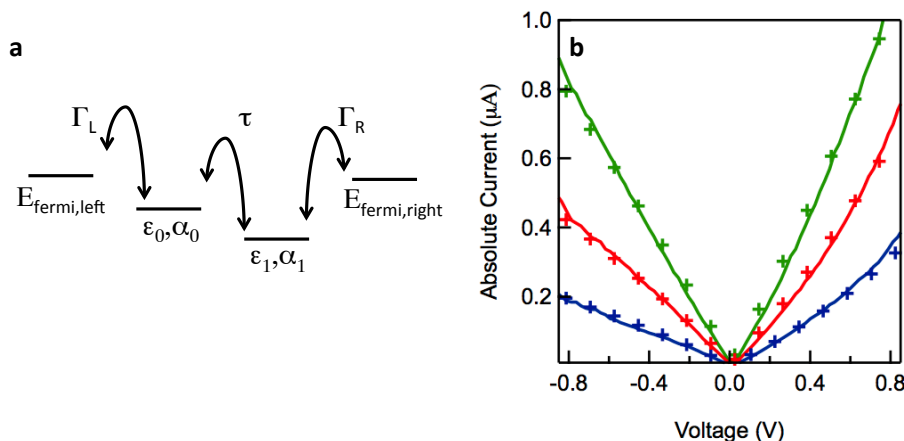


**Figure S8: Tight binding model for rectifiers.** **a** Two site tight-binding model to identify parameters controlling rectification. See text for parameter definitions **b** IV curves for molecules **1,2** and **3** (solid lines). Overlaid markers represent model IV curves that show good agreement with the data. Parameters for the model curves are listed in Table ST1.

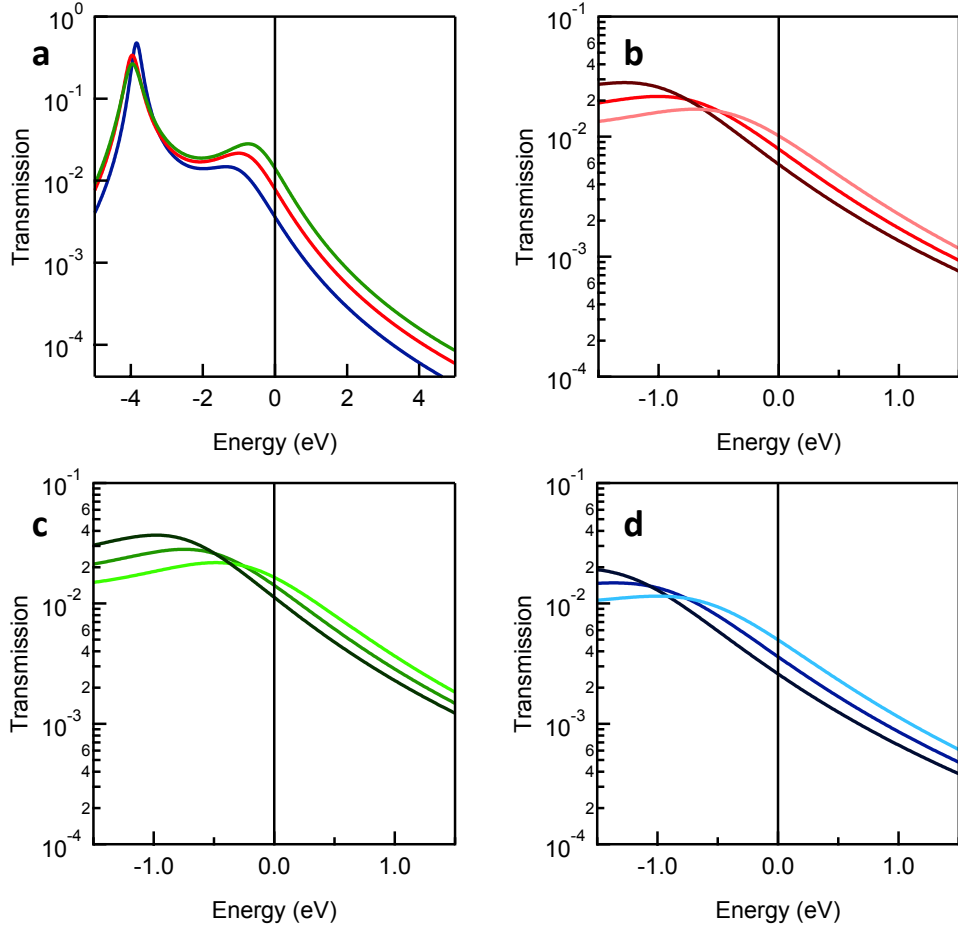


**Figure S9: Transmission Curves from Tight Binding.** **a** Zero-bias transmission functions,  $T(E, V=0V)$  calculated from the tight binding model described in Figure S4. Red, green and blue curves represented transmission functions calculated for molecules **1**, **2**, **3** respectively. **b,c,d** show a zoomed in view of  $T(E, 0V)$ , along with  $T(E, +1V)$  (lighter color) and  $T(E, -1V)$  (darker color). The gateway is seen to move with bias for all three biases, but is most prominent for figure **d**, which corresponds to molecule **3**. Thus, the model predicts highest rectification for this molecule

Variable	Molecule 1	Molecule 2	Molecule 3
$\Gamma_L$	2.1	2.1	2.1
$\epsilon_0$	-1.3	-1.3	-1.3
$\tau$	1.3	1.5	1.0
$\epsilon_1$	-3.4	-3.2	-3.5
$\Gamma_R$	.045	.045	.045
$\alpha_0$	-0.35	-0.35	-0.35
$\alpha_1$	0.05	0.10	0.00

**Table ST1: Parameters for tight binding model.** Parameters are defined in the text. Shaded cells show parameters that have been varied across molecules **1**, **2**, and **3**.  $\epsilon_1$ ,  $\tau$ ,  $\alpha_1$  are assumed to change systematically with coupling, with  $\epsilon_0$  coming closer to  $E_F$  with increasing coupling, and  $\tau$  and  $\alpha_1$  increasing with increasing coupling.

## 6. References

- (1) Meisner, J. S.; Sedbrook, D. F.; Krikorian, M.; Chen, J.; Sattler, A.; Carnes, M. E.; Murray, C. B.; Steigerwald, M.; Nuckolls, C. *Chemical Science*, **2012**, 3, 1007-1014.
- (2) Aradhya, S. V.; Meisner, J. S.; Krikorian, M.; Ahn, S.; Parameswaran, R.; Steigerwald, M. L.; Nuckolls, C.; Venkataraman, L. *Nano Lett.*, **2012**, 12, (3), 1643-1647.
- (3) Kondoh, A.; Yorimitsu, H.; Oshima, K. *Tetrahedron*, **2006**, 62, 2357-2360.
- (4) Wong, Y.-C.; Jayanth, T. T.; Cheng, C.-H. *Organic Letters*, **2006**, 8, 5613-5616.
- (5) Meisner, J. S.; Ahn, S.; Aradhya, S. V.; Krikorian, M.; Parameswaran, R.; Steigerwald, M.; Venkataraman, L.; Nuckolls, C. *Journal of the American Chemical Society*, **2012**, 134, 20440-20445.
- (6) Chen, W.; Widawsky, J. R.; Vazquez, H.; Schneebeli, S. T.; Hybertsen, M. S.; Breslow, R.; Venkataraman, L. *Journal of the American Chemical Society*, **2011**, 133, 17160-17163.
- (7) Yamamoto, T.; Takimiya, K. *Journal of the American Chemical Society*, **2007**, 129, 2224-2225.
- (8) Kamenetska, M.; Koentopp, M.; Whalley, A. C.; Park, Y. S.; Steigerwald, M. L.; Nuckolls, C.; Hybertsen, M. S.; Venkataraman, L. *Physical Review Letters*, **2009**, 102, (12).
- (9) Widawsky, J. R.; Kamenetska, M.; Klare, J.; Nuckolls, C.; Steigerwald, M. L.; Hybertsen, M. S.; Venkataraman, L. *Nanotechnology*, **2009**, 20, (43).
- (10) Ordejón, P.; Artacho, E.; Soler, J. M. *Phys. Rev. B*, **1996**, 53, (16), R10441.
- (11) Soler, J. M.; Artacho, E.; Gale, J. D.; García, A.; Junquera, J.; Ordejón, P.; Sánchez-Portal, D. *Journal of Physics: Condensed Matter*, **2002**, 14, (11), 2745.
- (12) Perdew, J. P.; Burke, K.; Ernzerhof, M. *Phys. Rev. Lett.*, **1996**, 77, (18), 3865-3868.
- (13) Park, Y. S.; Widawsky, J. R.; Kamenetska, M.; Steigerwald, M. L.; Hybertsen, M. S.; Nuckolls, C.; Venkataraman, L. *J. Am. Chem. Soc.*, **2009**, 131, (31), 10820-10821.
- (14) Choi, H. J.; Cohen, M. L.; Louie, S. G. *Phys. Rev. B*, **2007**, 76, (15), 155420.
- (15) Quek, S. Y.; Choi, H. J.; Louie, S. G.; Neaton, J. *Nano Lett*, **2009**, 9, (11), 3949-3953.
- (16) Quek, S. Y.; Venkataraman, L.; Choi, H. J.; Louie, S. G.; Hybertsen, M. S.; Neaton, J. *Nano Lett*, **2007**, 7, (11), 3477-3482.
- (17) Darancet, P.; Widawsky, J. R.; Choi, H. J.; Venkataraman, L.; Neaton, J. B. *Nano Lett.*, **2012**, 12, (12), 6250-6254.
- (18) Quek, S. Y.; Kamenetska, M.; Steigerwald, M. L.; Choi, H. J.; Louie, S. G.; Hybertsen, M. S.; Neaton, J.; Venkataraman, L. *Nature nanotechnology*, **2009**, 4, (4), 230-234.
- (19) Datta, S., *Electronic transport in mesoscopic systems*. Cambridge university press: 1997.
- (20) Widawsky, J. R.; Chen, W.; Vázquez, H.; Kim, T.; Breslow, R.; Hybertsen, M. S.; Venkataraman, L. *Nano Lett*, **2013**.

## 6. Coordinates for DFT optimized Geometries

### Geometry Molecule 1

C 7.141179 11.675512 27.122999; C 7.345295 12.839966 26.327667; C 7.569237  
12.749445 24.943057; C 7.598807 11.477847 24.326246; C 7.375890 10.304311  
25.088759; C 7.154051 10.405982 26.467526; H 7.335596 13.835112 26.813461; H  
7.737394 13.658785 24.334137; S 7.980552 11.414323 22.574889; H 7.377431  
9.314280 24.590604; H 6.990415 9.478752 27.047695; C 9.702734 10.790320  
22.668466; H 9.752059 9.846920 23.252200; H 10.034742 10.610240 21.617748; H  
10.328594 11.584317 23.131386; C 6.929384 11.829304 28.562346; C 6.678106  
10.807145 29.445562; H 6.622218 9.771009 29.052934; H 6.979812 12.870753  
28.940095; C 6.461080 10.919557 30.881510; C 6.191839 9.729171 31.622205; C  
5.962494 9.764540 33.001107; C 5.988598 11.002095 33.713827; C 6.272824  
12.194199 32.974600; C 6.495776 12.156375 31.596675; H 5.749356 8.826865  
33.550761; H 6.157576 8.761185 31.084386; H 6.695516 13.102931 31.059247; H  
6.298685 13.163179 33.510730; C 5.694789 11.056473 35.153556; H 5.352158  
12.046937 35.521223; H 5.046379 10.232301 35.520597; Au 6.735287 9.547049  
21.447757; Au 9.084605 8.237812 36.296484; Au 5.136797 7.180814 21.410211; Au  
10.425748 10.776673 36.276111; Au 8.004386 6.948160 21.400282; Au 7.530660  
10.702449 36.199328; Au 2.039447 5.304592 19.291594; Au 13.553761 12.558785  
38.425186; Au 3.450120 7.915061 19.269469; Au 12.116785 9.956391 38.438691; Au  
4.996944 5.222956 19.300158; Au 10.591723 12.651667 38.391998; Au 6.551218  
7.929617 19.069316; Au 9.021885 9.982401 38.610721; Au 8.059363 5.179320  
19.222461; Au 7.542908 12.626519 38.423296; Au 9.608151 7.897223 19.248523; Au  
5.984730 9.944319 38.519525; Au 11.032424 5.296075 19.281062; Au 4.549456  
12.566798 38.480513; Au 12.496228 7.895965 19.279482; Au 3.085091 9.969595  
38.436727; Au 2.029606 10.505896 19.278083; Au 13.574803 7.370228 38.423275; Au  
3.514550 13.051634 19.300556; Au 12.100589 4.794739 38.408267; Au 4.981253  
10.512513 19.305112; Au 10.636366 7.306870 38.448409; Au 6.518447 13.025507

19.238056; Au 9.058053 4.818304 38.410209; Au 8.106191 10.534689 19.106536; Au 7.485869 7.300817 38.429086; Au 9.575791 13.045979 19.246370; Au 6.029773 4.783094 38.418245; Au 11.058023 10.492160 19.221176; Au 4.545291 7.361325 38.430108; Au 12.510052 13.078051 19.299820; Au 3.093416 4.793639 38.391488; Au 2.061773 3.582141 16.785014; Au 13.536722 14.291541 40.920516; Au 3.555006 6.166866 16.791465; Au 12.029735 11.711680 40.911229; Au 5.029525 3.576828 16.786457; Au 10.552839 14.296249 40.889728; Au 6.523334 6.132286 16.782520; Au 9.061418 11.730277 40.921269; Au 8.025774 3.553902 16.763432; Au 7.566356 14.302382 40.902042; Au 9.518177 6.147026 16.767738; Au 6.086393 11.720064 40.931877; Au 11.025555 3.582166 16.764853; Au 4.578737 14.304763 40.939870; Au 12.507944 6.157365 16.784486; Au 3.081533 11.708153 40.936124; Au 2.056985 8.743006 16.786881; Au 13.519666 9.124132 40.914537; Au 3.548901 11.328622 16.790552; Au 12.039375 6.541178 40.912416; Au 5.024888 8.744389 16.750989; Au 10.552032 9.122374 40.938238; Au 6.510561 11.312294 16.741413; Au 9.063479 6.545138 40.926691; Au 8.035650 8.719902 16.723250; Au 7.563274 9.115922 40.943452; Au 9.540191 11.333282 16.712353; Au 6.077375 6.543931 40.915900; Au 11.010325 8.730852 16.763469; Au 4.573386 9.124892 40.939212; Au 12.518886 11.334993 16.751663; Au 3.086070 6.536765 40.940413; Au 2.064822 1.818624 14.319555; Au 13.525726 16.056985 43.368540; Au 3.552991 4.401676 14.333613; Au 12.038009 13.473681 43.361546; Au 5.033005 1.814431 14.327458; Au 10.551942 16.050479 43.362615; Au 6.530825 4.397653 14.330136; Au 9.062157 13.471492 43.355106; Au 8.024249 1.811136 14.311237; Au 7.569235 16.053159 43.360688; Au 9.517855 4.388296 14.323052; Au 6.081986 13.475897 43.367979; Au 11.022302 1.816542 14.307470; Au 4.587934 16.059406 43.377756; Au 12.509851 4.401605 14.319167; Au 3.087288 13.474552 43.379261; Au 2.059275 6.983934 14.329672; Au 13.529858 10.888002 43.369188; Au 3.550373 9.567489 14.324620; Au 12.040771 8.301685 43.378281; Au 5.042502 6.974684 14.316784; Au 10.552560 10.890480 43.373032; Au 6.529978 9.562390 14.304206; Au 9.059920 8.300394 43.382099; Au 8.024563 6.965264 14.310598; Au 7.569171 10.892304 43.380064; Au 9.518719 9.554467 14.308317; Au 6.079112 8.305786 43.375035; Au 11.016370 6.975748 14.323665; Au 4.584741 10.890973 43.374586; Au 12.507774 9.561115 14.326011; Au

3.086471 8.311966 43.365152; Au 2.063950 0.030650 11.872356; Au 13.537920  
 17.828870 45.818831; Au 3.555950 2.614860 11.872356; Au 12.045920 15.244660  
 45.818831; Au 2.063950 5.199070 11.872356; Au 13.537920 12.660450 45.818831; Au  
 3.555950 7.783280 11.872356; Au 12.045920 10.076240 45.818831; Au 5.047940  
 0.030650 11.872356; Au 10.553930 17.828870 45.818831; Au 6.539940 2.614860  
 11.872356; Au 9.061930 15.244660 45.818831; Au 5.047940 5.199070 11.872356; Au  
 10.553930 12.660450 45.818831; Au 6.539940 7.783280 11.872356; Au 9.061930  
 10.076240 45.818831; Au 8.031930 0.030650 11.872356; Au 7.569930 17.828870  
 45.818831; Au 9.523930 2.614860 11.872356; Au 6.077940 15.244660 45.818831; Au  
 8.031930 5.199070 11.872356; Au 7.569930 12.660450 45.818831; Au 9.523930  
 7.783280 11.872356; Au 6.077940 10.076240 45.818831; Au 11.015930 0.030650  
 11.872356; Au 4.585940 17.828870 45.818831; Au 12.507920 2.614860 11.872356; Au  
 3.093950 15.244660 45.818831; Au 11.015930 5.199070 11.872356; Au 4.585940  
 12.660450 45.818831; Au 12.507920 7.783280 11.872356; Au 3.093950 10.076240  
 45.818831; Au 2.063950 -1.692160 9.435936; Au 13.537920 19.551680 48.255241; Au  
 3.555950 0.892050 9.435936; Au 12.045920 16.967470 48.255241; Au 2.063950  
 3.476260 9.435936; Au 13.537920 14.383260 48.255241; Au 3.555950 6.060470  
 9.435936; Au 12.045920 11.799050 48.255241; Au 5.047940 -1.692160 9.435936; Au  
 10.553930 19.551680 48.255241; Au 6.539940 0.892050 9.435936; Au 9.061930  
 16.967470 48.255241; Au 5.047940 3.476260 9.435936; Au 10.553930 14.383260  
 48.255241; Au 6.539940 6.060470 9.435936; Au 9.061930 11.799050 48.255241; Au  
 8.031930 -1.692160 9.435936; Au 7.569930 19.551680 48.255241; Au 9.523930  
 0.892050 9.435936; Au 6.077940 16.967470 48.255241; Au 8.031930 3.476260  
 9.435936; Au 7.569930 14.383260 48.255241; Au 9.523930 6.060470 9.435936; Au  
 6.077940 11.799050 48.255241; Au 11.015930 -1.692160 9.435936; Au 4.585940  
 19.551680 48.255241; Au 12.507920 0.892050 9.435936; Au 3.093950 16.967470  
 48.255241; Au 11.015930 3.476260 9.435936; Au 4.585940 14.383260 48.255241; Au  
 12.507920 6.060470 9.435936; Au 3.093950 11.799050 48.255241; Au 2.063950 -  
 3.414970 6.999516; Au 13.537920 21.274490 50.691661; Au 3.555950 -0.830760  
 6.999516; Au 12.045920 18.690280 50.691661; Au 2.063950 1.753460 6.999516; Au  
 13.537920 16.106070 50.691661; Au 3.555950 4.337670 6.999516; Au 12.045920

13.521850 50.691661; Au 5.047940 -3.414970 6.999516; Au 10.553930 21.274490 50.691661; Au 6.539940 -0.830760 6.999516; Au 9.061930 18.690280 50.691661; Au 5.047940 1.753460 6.999516; Au 10.553930 16.106070 50.691661; Au 6.539940 4.337670 6.999516; Au 9.061930 13.521850 50.691661; Au 8.031930 -3.414970 6.999516; Au 7.569930 21.274490 50.691661; Au 9.523930 -0.830760 6.999516; Au 6.077940 18.690280 50.691661; Au 8.031930 1.753460 6.999516; Au 7.569930 16.106070 50.691661; Au 9.523930 4.337670 6.999516; Au 6.077940 13.521850 50.691661; Au 11.015930 -3.414970 6.999516; Au 4.585940 21.274490 50.691661; Au 12.507920 -0.830760 6.999516; Au 3.093950 18.690280 50.691661; Au 11.015930 1.753460 6.999516; Au 4.585940 16.106070 50.691661; Au 12.507920 4.337670 6.999516; Au 3.093950 13.521850 50.691661;

Geometry for Molecule 1 with C-S-C-C constrained to 90-degree angle

C 5.569665 16.616180 27.097002; S 5.933033 16.511311 25.310923; C 7.761008 16.440166 25.398867; H 8.082706 15.621527 26.017506; H 8.111691 16.319712 24.403553; H 8.107494 17.368851 25.811869; C 5.105967 16.812042 29.892396; C 5.314565 17.975918 29.095683; C 5.536702 17.889080 27.709491; C 5.346822 15.444207 27.857834; C 5.117204 15.544523 29.236559; H 5.300854 18.971340 29.581394; H 5.690441 18.804491 27.105492; H 5.358137 14.455624 27.357106; H 4.951876 14.616251 29.814316; C 4.892148 16.964881 31.333252; C 4.647176 15.942632 32.218202; H 4.595716 14.905370 31.827500; H 4.937558 18.006768 31.710574; C 4.430590 16.056130 33.655491; C 4.156247 14.869746 34.400609; C 3.927464 14.910698 35.780301; C 3.960024 16.150637 36.488387; C 4.245580 17.339164 35.744541; C 4.469779 17.295010 34.367137; H 3.709566 13.976382 36.333784; H 4.118482 13.898786 33.868092; H 4.677116 18.238534 33.828202; H 4.275779 18.309278 36.278031; C 3.681393 16.214748 37.930267; H 3.325155 17.202169 38.293268; H 3.054788 15.382553 38.317160; Au 5.298936 14.301407 24.294800; Au 7.138200 13.490435 39.029683; Au 3.899009 11.902789 24.069471; Au 8.448408 16.045027 39.004542; Au 6.795019 11.857870 24.082787; Au 5.552538 15.927264 38.934630; Au -1.944125 15.412205 21.930451; Au 11.600706 17.857260 41.153451; Au -0.448705 18.013419 21.943367; Au 10.161530 15.254348 41.166883;

Au 0.986143 15.451544 21.932959; Au 8.636165 17.936949 41.105496; Au 2.495838  
17.985867 21.946421; Au 7.065201 15.255957 41.342908; Au 3.950171 15.462230  
21.936807; Au 5.595383 17.903254 41.132151; Au 5.534224 17.951151 21.922395; Au  
4.023472 15.232005 41.264459; Au 7.024775 15.413564 21.896950; Au 2.597499  
17.862746 41.204919; Au 8.551071 17.955931 21.906841; Au 1.126534 15.268149  
41.169015; Au -1.907414 20.566902 21.932829; Au 11.621006 12.668832 41.152093;  
Au -0.496859 23.174966 21.942610; Au 10.145999 10.084946 41.132782; Au 1.039814  
20.586182 21.943828; Au 8.688588 12.597220 41.189844; Au 2.388868 23.212705  
21.902824; Au 7.104924 10.104686 41.119813; Au 4.006745 20.454157 21.894279; Au  
5.529089 12.584845 41.165935; Au 5.451828 23.207241 21.780818; Au 4.080447  
10.066730 41.137237; Au 7.074996 20.451457 21.903030; Au 2.592768 12.655495  
41.161206; Au 8.535174 23.150448 21.998911; Au 1.142145 10.094764 41.121035; Au  
-1.957087 13.693565 19.465726; Au 11.585915 19.569392 43.638971; Au -0.450405  
16.293710 19.436471; Au 10.075248 16.991368 43.627996; Au 1.033228 13.713091  
19.442259; Au 8.600390 19.572353 43.600653; Au 2.533952 16.297097 19.446416; Au  
7.111207 17.003318 43.637785; Au 4.014302 13.711207 19.424519; Au 5.619336  
19.576196 43.609354; Au 5.520108 16.275840 19.437130; Au 4.140271 16.998207  
43.649138; Au 7.014862 13.687007 19.443910; Au 2.630166 19.582381 43.655699; Au  
8.508617 16.282258 19.428791; Au 1.132085 16.988000 43.653604; Au -1.924529  
18.883115 19.434527; Au 11.566727 14.406035 43.635782; Au -0.435871 21.461870  
19.454581; Au 10.091900 11.817855 43.634315; Au 1.054309 18.885212 19.444583; Au  
8.602620 14.397759 43.660864; Au 2.551458 21.469044 19.447738; Au 7.112564  
11.819677 43.644779; Au 4.039164 18.867478 19.438252; Au 5.613174 14.387795  
43.668269; Au 5.523788 21.447474 19.458877; Au 4.124629 11.817316 43.635963; Au  
7.024265 18.869301 19.434526; Au 2.620553 14.402069 43.662693; Au 8.508652  
21.462613 19.454660; Au 1.134574 11.815824 43.656994; Au -1.924734 11.988067  
17.017257; Au 11.578537 21.300497 46.070852; Au -0.442219 14.566891 17.015931;  
Au 10.089734 18.716114 46.062691; Au 1.053759 11.987575 17.013247; Au 8.605515  
21.290146 46.063164; Au 2.549683 14.571878 17.010791; Au 7.114794 18.716768  
46.055293; Au 4.042746 11.983019 17.000468; Au 5.620966 21.293134 46.061928; Au  
5.533529 14.573554 17.004937; Au 4.136076 18.720656 46.067626; Au 7.023061

11.980297 17.006748; Au 2.639007 21.303750 46.078443; Au 8.510779 14.563161  
17.014554; Au 1.140502 18.718782 46.080981; Au -1.926313 17.156389 17.006571; Au  
11.582513 16.132622 46.072199; Au -0.431770 19.743584 17.001981; Au 10.092269  
13.544756 46.083207; Au 1.055279 17.155576 17.010099; Au 8.604935 16.135383  
46.078721; Au 2.551175 19.738773 17.012908; Au 7.112646 13.540164 46.088595; Au  
4.037941 17.154844 17.012734; Au 5.622077 16.136942 46.084250; Au 5.533522  
19.744787 17.011698; Au 4.132019 13.546836 46.080726; Au 7.025022 17.155408  
17.010727; Au 2.638057 16.136240 46.077025; Au 8.517596 19.738982 17.008417; Au  
1.138303 13.557387 46.070554; Au -1.922789 10.256833 14.576839; Au 11.591079  
23.030962 48.505604; Au -0.431579 12.838028 14.576839; Au 10.099855 20.449766  
48.505604; Au 1.059748 10.256833 14.576839; Au 8.608506 23.030962 48.505604; Au  
2.552664 12.838028 14.576839; Au 7.115601 20.449766 48.505604; Au 4.045244  
10.256833 14.576839; Au 5.623063 23.030962 48.505604; Au 5.536546 12.838028  
14.576839; Au 4.131707 20.449766 48.505604; Au 7.027667 10.256833 14.576839; Au  
2.640587 23.030962 48.505604; Au 8.520045 12.838028 14.576839; Au 1.148236  
20.449766 48.505604; Au -1.922789 15.419224 14.576839; Au 11.591079 17.868572  
48.505604; Au -0.431579 18.000420 14.576839; Au 10.099855 15.284012 48.505604;  
Au 1.059748 15.419224 14.576839; Au 8.608506 17.868572 48.505604; Au 2.552664  
18.000420 14.576839; Au 7.115601 15.284012 48.505604; Au 4.045244 15.419224  
14.576839; Au 5.623063 17.868572 48.505604; Au 5.536546 18.000420 14.576839; Au  
4.131707 15.284012 48.505604; Au 7.027667 15.419224 14.576839; Au 2.640587  
17.868572 48.505604; Au 8.520045 18.000420 14.576839; Au 1.148236 15.284012  
48.505604; Au -1.922789 8.534025 12.140421; Au 11.591079 24.753769 50.942013; Au  
-0.431579 11.115221 12.140421; Au 10.099855 22.172575 50.942013; Au 1.059748  
8.534025 12.140421; Au 8.608506 24.753769 50.942013; Au 2.552664 11.115221  
12.140421; Au 7.115601 22.172575 50.942013; Au 4.045244 8.534025 12.140421; Au  
5.623063 24.753769 50.942013; Au 5.536546 11.115221 12.140421; Au 4.131707  
22.172575 50.942013; Au 7.027667 8.534025 12.140421; Au 2.640587 24.753769  
50.942013; Au 8.520045 11.115221 12.140421; Au 1.148236 22.172575 50.942013; Au  
-1.922789 13.696415 12.140421; Au 11.591079 19.591379 50.942013; Au -0.431579  
16.277611 12.140421; Au 10.099855 17.006819 50.942013; Au 1.059748 13.696415

12.140421; Au 8.608506 19.591379 50.942013; Au 2.552664 16.277611 12.140421; Au  
 7.115601 17.006819 50.942013; Au 4.045244 13.696415 12.140421; Au 5.623063  
 19.591379 50.942013; Au 5.536546 16.277611 12.140421; Au 4.131707 17.006819  
 50.942013; Au 7.027667 13.696415 12.140421; Au 2.640587 19.591379 50.942013; Au  
 8.520045 16.277611 12.140421; Au 1.148236 17.006819 50.942013; Au -1.922789  
 6.811218 9.704003; Au 11.591079 26.476578 53.378429; Au -0.431579 9.392413  
 9.704003; Au 10.099855 23.895382 53.378429; Au 1.059748 6.811218 9.704003; Au  
 8.608506 26.476578 53.378429; Au 2.552664 9.392413 9.704003; Au 7.115601  
 23.895382 53.378429; Au 4.045244 6.811218 9.704003; Au 5.623063 26.476578  
 53.378429; Au 5.536546 9.392413 9.704003; Au 4.131707 23.895382 53.378429; Au  
 7.027667 6.811218 9.704003; Au 2.640587 26.476578 53.378429; Au 8.520045  
 9.392413 9.704003; Au 1.148236 23.895382 53.378429; Au -1.922789 11.973608  
 9.704003; Au 11.591079 21.314188 53.378429; Au -0.431579 14.554803 9.704003; Au  
 10.099855 18.729628 53.378429; Au 1.059748 11.973608 9.704003; Au 8.608506  
 21.314188 53.378429; Au 2.552664 14.554803 9.704003; Au 7.115601 18.729628  
 53.378429; Au 4.045244 11.973608 9.704003; Au 5.623063 21.314188 53.378429; Au  
 5.536546 14.554803 9.704003; Au 4.131707 18.729628 53.378429; Au 7.027667  
 11.973608 9.704003; Au 2.640587 21.314188 53.378429; Au 8.520045 14.554803  
 9.704003; Au 1.148236 18.729628 53.378429

Geometry for Molecule 1 with C-S-C-C angle constrained to 0-degrees

C 5.569665 16.616180 27.097002; S 5.933033 16.511311 25.310923; C 5.919171  
 14.709676 25.118580; H 5.004649 14.298120 25.473722; H 6.042562 14.512744  
 24.093811; H 6.787983 14.291023 25.672664; C 5.110726 16.845559 29.909212; C  
 5.328899 17.996532 29.094009; C 5.556642 17.893096 27.710738; C 5.348056  
 15.459821 27.887038; C 5.124585 15.577169 29.263309; H 5.322640 18.998582  
 29.566008; H 5.725317 18.805760 27.106684; H 5.356454 14.449623 27.446101; H  
 4.964731 14.649759 29.843688; C 4.892964 16.993316 31.347739; C 4.648400  
 15.962297 32.225379; H 4.599767 14.927341 31.828263; H 4.934387 18.032383  
 31.732641; C 4.430456 16.064898 33.661648; C 4.157250 14.874762 34.403169; C  
 3.927501 14.911369 35.781949; C 3.957790 16.149931 36.494131; C 4.243608

17.341166 35.754165; C 4.468615 17.301177 34.378065; H 3.710301 13.975396  
 36.333419; H 4.121350 13.904864 33.867929; H 4.676478 18.245670 33.840984; H  
 4.273052 18.309726 36.290528; C 3.676965 16.211286 37.934172; H 3.323622  
 17.198852 38.299823; H 3.053031 15.378228 38.322124; Au 2.580030 19.776266  
 24.059090; Au 7.136377 13.485090 39.029975; Au 1.132141 17.280752 24.064166; Au  
 8.447971 16.040073 39.003753; Au 4.010342 17.266752 23.926422; Au 5.552504  
 15.922871 38.933279; Au -1.936828 15.433576 21.927431; Au 11.601705 17.859734  
 41.154119; Au -0.527439 18.043163 21.896239; Au 10.161643 15.256623 41.166859;  
 Au 1.028900 15.351390 21.979084; Au 8.636925 17.935954 41.103142; Au 2.547706  
 18.048733 21.694532; Au 7.065165 15.255276 41.341829; Au 4.049729 15.338765  
 21.811094; Au 5.598564 17.904508 41.127755; Au 5.654645 18.075803 21.761217; Au  
 4.025227 15.235341 41.264311; Au 7.070577 15.442557 21.805094; Au 2.599090  
 17.865146 41.203684; Au 8.529949 18.025000 21.928958; Au 1.127403 15.270092  
 41.166905; Au -1.954397 20.631255 21.938348; Au 11.621227 12.670135 41.150744;  
 Au -0.475102 23.202843 21.952085; Au 10.145295 10.085588 41.131862; Au 0.975202  
 20.685062 21.916041; Au 8.688373 12.597886 41.190232; Au 2.552077 23.158302  
 21.954263; Au 7.105836 10.105031 41.114995; Au 4.145622 20.686896 21.903294; Au  
 5.529516 12.584687 41.167600; Au 5.593167 23.196987 21.865015; Au 4.082011  
 10.066454 41.136809; Au 7.088012 20.638436 21.921141; Au 2.593528 12.657269  
 41.159218; Au 8.529001 23.204542 21.952814; Au 1.142358 10.096819 41.120929; Au  
 -1.916280 13.720989 19.442363; Au 11.586232 19.571987 43.638853; Au -0.412812  
 16.294123 19.452445; Au 10.075722 16.993358 43.627767; Au 1.062262 13.714483  
 19.482773; Au 8.600614 19.573606 43.598430; Au 2.536000 16.283652 19.404983; Au  
 7.111571 17.005184 43.636722; Au 4.036375 13.679190 19.414258; Au 5.620429  
 19.576695 43.606201; Au 5.530646 16.287883 19.389779; Au 4.141525 17.000816  
 43.647807; Au 7.039654 13.704743 19.394925; Au 2.631108 19.584189 43.654831; Au  
 8.546775 16.311625 19.406505; Au 1.133177 16.990168 43.652037; Au -1.910625  
 18.890750 19.439738; Au 11.567551 14.407786 43.634116; Au -0.430633 21.472653  
 19.451819; Au 10.092824 11.818988 43.633722; Au 1.044782 18.893949 19.411279; Au  
 8.602992 14.399339 43.660277; Au 2.544987 21.452638 19.439281; Au 7.113153  
 11.819723 43.644095; Au 4.046829 18.892946 19.386496; Au 5.613876 14.389283

43.669285; Au 5.544177 21.447220 19.422627; Au 4.125157 11.818088 43.635575; Au 7.066627 18.895009 19.387979; Au 2.621523 14.403630 43.661121; Au 8.535250 21.478609 19.423136; Au 1.135300 11.817703 43.655747; Au -1.914186 11.991726 17.010373; Au 11.579307 21.301126 46.070603; Au -0.426024 14.568751 17.018973; Au 10.090381 18.716882 46.062324; Au 1.057699 11.993919 17.025097; Au 8.606204 21.290326 46.061959; Au 2.542524 14.563808 17.011428; Au 7.115209 18.717305 46.053978; Au 4.039148 11.978793 17.005019; Au 5.621583 21.293267 46.060699; Au 5.530061 14.561048 16.993763; Au 4.136352 18.721428 46.066879; Au 7.027871 11.979969 16.996093; Au 2.639375 21.303994 46.077671; Au 8.530877 14.569654 16.994716; Au 1.141160 18.718999 46.079938; Au -1.912698 17.158508 17.004616; Au 11.583363 16.132939 46.070671; Au -0.428822 19.746124 17.000183; Au 10.093290 13.545503 46.082415; Au 1.053797 17.151546 16.991577; Au 8.605324 16.135305 46.077937; Au 2.542796 19.744661 16.985065; Au 7.113521 13.539968 46.087986; Au 4.038486 17.148574 16.986099; Au 5.622612 16.137482 46.083773; Au 5.534570 19.734374 16.987410; Au 4.132090 13.547485 46.080344; Au 7.030833 17.151268 16.992428; Au 2.638693 16.136507 46.075738; Au 8.535422 19.738400 16.994485; Au 1.139125 13.557751 46.068670; Au -1.922789 10.256833 14.576839; Au 11.591079 23.030962 48.505604; Au -0.431579 12.838028 14.576839; Au 10.099855 20.449766 48.505604; Au 1.059748 10.256833 14.576839; Au 8.608506 23.030962 48.505604; Au 2.552664 12.838028 14.576839; Au 7.115601 20.449766 48.505604; Au 4.045244 10.256833 14.576839; Au 5.623063 23.030962 48.505604; Au 5.536546 12.838028 14.576839; Au 4.131707 20.449766 48.505604; Au 7.027667 10.256833 14.576839; Au 2.640587 23.030962 48.505604; Au 8.520045 12.838028 14.576839; Au 1.148236 20.449766 48.505604; Au -1.922789 15.419224 14.576839; Au 11.591079 17.868572 48.505604; Au -0.431579 18.000420 14.576839; Au 10.099855 15.284012 48.505604; Au 1.059748 15.419224 14.576839; Au 8.608506 17.868572 48.505604; Au 2.552664 18.000420 14.576839; Au 7.115601 15.284012 48.505604; Au 4.045244 15.419224 14.576839; Au 5.623063 17.868572 48.505604; Au 5.536546 18.000420 14.576839; Au 4.131707 15.284012 48.505604; Au 7.027667 15.419224 14.576839; Au 2.640587 17.868572 48.505604; Au 8.520045 18.000420 14.576839; Au 1.148236 15.284012 48.505604; Au -1.922789 8.534025 12.140421; Au 11.591079 24.753769 50.942013; Au

-0.431579 11.115221 12.140421; Au 10.099855 22.172575 50.942013; Au 1.059748  
8.534025 12.140421; Au 8.608506 24.753769 50.942013; Au 2.552664 11.115221  
12.140421; Au 7.115601 22.172575 50.942013; Au 4.045244 8.534025 12.140421; Au  
5.623063 24.753769 50.942013; Au 5.536546 11.115221 12.140421; Au 4.131707  
22.172575 50.942013; Au 7.027667 8.534025 12.140421; Au 2.640587 24.753769  
50.942013; Au 8.520045 11.115221 12.140421; Au 1.148236 22.172575 50.942013; Au  
-1.922789 13.696415 12.140421; Au 11.591079 19.591379 50.942013; Au -0.431579  
16.277611 12.140421; Au 10.099855 17.006819 50.942013; Au 1.059748 13.696415  
12.140421; Au 8.608506 19.591379 50.942013; Au 2.552664 16.277611 12.140421; Au  
7.115601 17.006819 50.942013; Au 4.045244 13.696415 12.140421; Au 5.623063  
19.591379 50.942013; Au 5.536546 16.277611 12.140421; Au 4.131707 17.006819  
50.942013; Au 7.027667 13.696415 12.140421; Au 2.640587 19.591379 50.942013; Au  
8.520045 16.277611 12.140421; Au 1.148236 17.006819 50.942013; Au -1.922789  
6.811218 9.704003; Au 11.591079 26.476578 53.378429; Au -0.431579 9.392413  
9.704003; Au 10.099855 23.895382 53.378429; Au 1.059748 6.811218 9.704003; Au  
8.608506 26.476578 53.378429; Au 2.552664 9.392413 9.704003; Au 7.115601  
23.895382 53.378429; Au 4.045244 6.811218 9.704003; Au 5.623063 26.476578  
53.378429; Au 5.536546 9.392413 9.704003; Au 4.131707 23.895382 53.378429; Au  
7.027667 6.811218 9.704003; Au 2.640587 26.476578 53.378429; Au 8.520045  
9.392413 9.704003; Au 1.148236 23.895382 53.378429; Au -1.922789 11.973608  
9.704003; Au 11.591079 21.314188 53.378429; Au -0.431579 14.554803 9.704003; Au  
10.099855 18.729628 53.378429; Au 1.059748 11.973608 9.704003; Au 8.608506  
21.314188 53.378429; Au 2.552664 14.554803 9.704003; Au 7.115601 18.729628  
53.378429; Au 4.045244 11.973608 9.704003; Au 5.623063 21.314188 53.378429; Au  
5.536546 14.554803 9.704003; Au 4.131707 18.729628 53.378429; Au 7.027667  
11.973608 9.704003; Au 2.640587 21.314188 53.378429; Au 8.520045 14.554803  
9.704003; Au 1.148236 18.729628 53.378429;

## 8. NMR Spectra

